crystals

MDPI

Article

Investigation of the Processes of Structure Formation during Explosion Welding of Copper and Molybdenum

Fedor M. Noskov [1,*], Lyudmila I. Kveglis [1], Vyacheslav I. Mali [2], Maksim A. Esikov [2] and Rimma Y. Sakenova [3]

[1] Department of Materials Science and Materials Processing Technologies, Polytechnic Institute, Siberian Federal University, 79 Svobodny Ave., Krasnoyarsk 660074, Russia; kveglis@list.ru
[2] Lavrentiev Institute of Hydrodynamics SB RAS, 15 Ak. Lavrentiev Ave., Novosibirsk 630090, Russia; esmax@ya.ru (M.A.E.)
[3] Physics Department, Sarsen Amanzholov East Kazakhstan University, 55 Kazakhstan St., Ust-Kamenogorsk 070000, Kazakhstan
* Correspondence: fnoskov@sfu-kras.ru

Abstract: This article examines the processes of structure formation occurring during joint plastic deformation by the explosion of copper and molybdenum. These components are dissimilar metals with very limited mutual solubility under normal conditions, and the circumstances allowing for their interaction, as well as the products of the mechanochemical reactions of such interactions, have not been sufficiently studied and require new approaches. A cluster approach was used to describe the processes of structure formation, which describes phase formation as the process transitioning of the polyhedron of the initial phase into the polyhedron of the final phase. This work shows that under the conditions under consideration, not only is the formation of solid solutions in the contact zone with smooth concentration transitions from one component to another possible, but also the formation of new structural states, which can be represented as localized icosahedral atomic configurations (amorphous metal clusters). Such a structure is capable of locally strengthening the composite, which is confirmed by microhardness studies.

Keywords: copper–molybdenum; plastic deformation; explosion welding; solid solutions; icosahedral phases; clusters

Citation: Noskov, F.M.; Kveglis, L.I.; Mali, V.I.; Esikov, M.A.; Sakenova, R.Y. Investigation of the Processes of Structure Formation during Explosion Welding of Copper and Molybdenum. *Crystals* **2023**, *13*, 1514. https://doi.org/10.3390/cryst13101514

Academic Editors: Małgorzata Hołyńska and Ionut Tranca

Received: 21 September 2023
Revised: 13 October 2023
Accepted: 17 October 2023
Published: 19 October 2023

1. Introduction

The Cu–Mo state diagram is currently only constructed by the calculation method since copper and molybdenum practically do not mix in liquid and solid states [1]. The effect of production technology on the structure and mechanical properties of composite materials made of molybdenum and copper has not been sufficiently studied [2]. Among the known methods of welding in a solid state, friction stir welding [3], diffusion welding [4], and explosion welding [5] are used. Considering the significant difference in mechanical properties between copper and molybdenum, explosion welding is the most productive. Therefore, it is relevant to study the effect of explosion welding of copper and molybdenum on the processes of structure formation in a layered copper–molybdenum composite, including the method of cluster modeling.

The study of the properties of composites and physico-chemical processes occurring during explosion welding makes it possible to obtain materials with unique properties, which opens up new opportunities for solving urgent problems [6,7]. A group of composite materials (CMs) consisting of dissimilar metals with limited mutual solubility is currently of particular interest since components such as composites combine a variety of properties that indicate a wide range of their possible uses. For example, composite materials based on copper and refractory metals have high strength characteristics and heat resistance. It is known [8] that with an increase in the volume of the refractory phase, the hardness of copper–molybdenum composites increases. By setting different thicknesses of the coating

layer from nitrides from 5 nm to 1000 nm and metals (Zr/Cr from 3.5 nm to 45 nm), the necessary final coating characteristics are ensured, such as impact strength, resistance to wear, and high-temperature oxidation.

As a result of this combined deposition, a coating hardness of 29–35 GPa is ensured, with a fairly low elastic modulus of 280–320 GPa. These are promising materials that can help open up new possibilities, for example, in the manufacture of electrodes for resistance welding [9].

The cluster modeling method is based on the representation of each structural state as a combination of elementary crystal clusters [10,11]. Cluster aggregates are a combination of elementary crystal clusters generated by simple (octahedron, tetrahedron) or more complex atomic configurations. The essence of the method lies in the fact that polymorphic transformation is described not as a relative displacement of flat atomic grids but as a reconstruction of three-dimensional coordination polyhedra that make up the crystal structures of phase partners in phase transformation [12,13]. The prototypes of clusters can be considered "unions" proposed by Laves to describe the structures of intermetallic phases [14], which are groups of atoms connected by the shortest lines [15,16].

New questions and problems have arisen in connection with the discovery of a new crystalline class of materials, the feature of which is icosahedral local atomic configurations [17,18]. In pure metals, the formation of distorted tetrahedra (for example, in an amorphous state) [19] cannot be explained by the size of atoms and is explained by a local change in the interatomic interaction potential caused by external causes (among which may be plastic deformation). For these reasons, in many metal alloys, the crystal structure may contain clusters with an icosahedral atomic configuration as building units.

Consisting only of tetrahedra, the objects have a high packing density, in which the packing density of the substance is 89%, which is significantly higher than the densest crystal packages of FCC and HCP with a density of 74%. The presence of such formations in the structure of molten or amorphous metal can explain their high density (for amorphous alloys, it is equal to 71–73% on average), while the estimated density of chaotic dense packing does not exceed 64–66% [20]. Since the packing density of amorphous alloys with icosahedral phases in fact turns out to be somewhat less than that of densely packed phases (FCC, HCP) and lattice BCC, it turns out that the metal in this state is more "loose". A systematic discussion of icosahedral formations in metals was conducted by Frank and Kasper [21,22], who showed the possibility of their formation and the main four types of clusters, one of which is a simple icosahedron. Currently, a large number of structures are known that belong to tetrahedrally densely packed phases and are formed in structurally unstable states characteristic of plastic deformation [23,24]. At the same time, amorphous alloys (metallic glasses) can be effectively used for reinforcing materials with a metal matrix [25].

There are known works in which it is shown that icosahedral phases can be obtained by the mechanochemical method [26,27]. We have shown the formation of tetrahedrally densely packed structures during plastic deformation in titanium nickelide [28], Gadfield steel [29], and iron [30]; however, icosahedral phases have not yet been found in systems with limited mutual solubility.

Thus, the aim of the work is to study the structural phase transformations that occur during joint plastic deformation in the copper–molybdenum system using the cluster approach.

2. Research Methodology

Composite material samples (CMs) were obtained by explosion welding of a multilayer package of technical copper plates (0.3 mm thick) and molybdenum plates (0.5 mm thick). A package of alternating seven copper and seven molybdenum plates was welded by explosion with a single charge of the explosive ammonite according to the method described in [31]. Ammonite was chosen as an explosive material. The horizontal collision point

velocity was estimated as 3600 m/s. Collision angles ranged from 24° (for upper plates) to 6.2° (for bottom plates).

In addition, experiments were carried out on a hydraulic press. Molybdenum wire with a diameter of 0.5 mm and a total length of 30 mm (experiment with wire 1) and 60 mm (experiment with wire 2) was divided into segments of about 1 mm and pressed into a copper plate with a thickness of 2 mm using a hydraulic press with a force of 3 tons. Also, a molybdenum plate with a size of 6 × 6 mm and a thickness of 1 mm was pressed into a copper plate with a thickness of 2 mm.

Throughout the course of this work, studies were carried out using an optical (Nikon Eclipse LV100) and a scanning electron microscope with an energy dispersion attachment (JEOL7001F), X-ray phase analysis (Bruker), as well as measuring the microhardness of samples (PMT-3).

3. Experimental Results

Figure 1 shows the structure of the copper–molybdenum composite material obtained by explosion welding. In the center of Figure 1, there is a layer of copper, above and below layers of molybdenum. The contact zone is well defined and has a wavy shape typical of this type of welding.

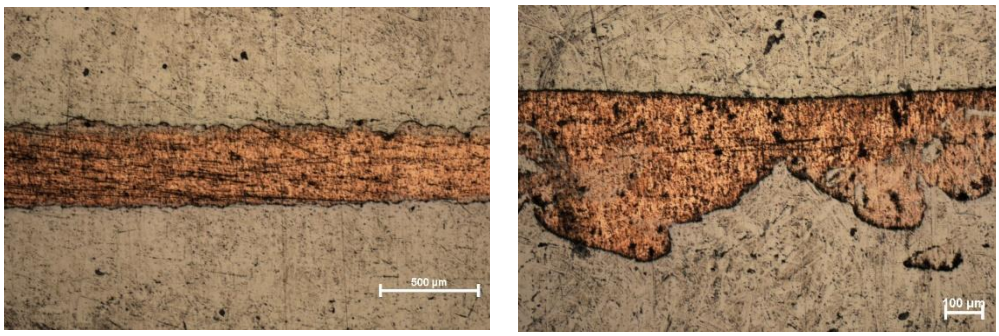

(**a**) (**b**)

Figure 1. The structure of the sample in the area of molybdenum and copper junction after explosion welding: (**a**)—normal interaction of components ×75; (**b**)—active interaction of components ×150.

It can be seen that the CM components interacted with each other with different intensities in different parts of the sample. Thus, active interaction and mixing of components took place in some areas (Figure 1b), which can be judged both by the blurred boundary of the transition zone and by visual signs—the color shades of the obtained solid solutions. This may indicate the occurrence of a solid–solution interaction, along with a purely mechanical one. In other areas, where the conditions of interaction were different, the intensity of mutual penetration of components was weak (Figure 1a).

Scanning electron microscopy makes it possible to study the local interaction of CM components in the transition zone. Several lines of spectra were constructed to study the depth of interpenetration of copper and molybdenum into each other. Figure 2a shows an electron microscopic image of a section of the copper–molybdenum transition zone from which a sequential series of spectra was taken. The results of this study are presented in Figure 2b.

It can be seen (Figure 2b) that in this local region, the depth of the transition zone of formation of solid solutions based on copper and molybdenum is about 10 microns. Thus, in the process of the solid–phase interaction, the mutual dissolution of copper in molybdenum and molybdenum in copper occurred.

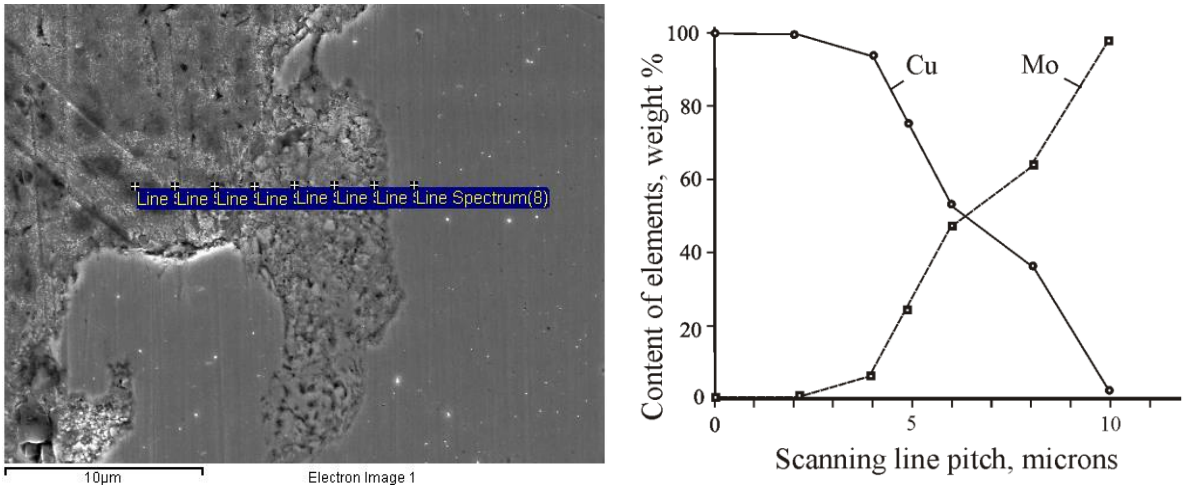

Figure 2. Electron microscopic examination of a copper–molybdenum CM sample: (**a**)—linear spectrum markers in the Cu–Mo transition zone; (**b**)—linear profile of copper and molybdenum concentrations.

To establish the phase composition of the obtained CM samples, layers of molybdenum and copper were separately examined using an X-ray diffractometer. Figure 3 shows X-ray diffractograms from molybdenum and copper layers obtained by explosion welding.

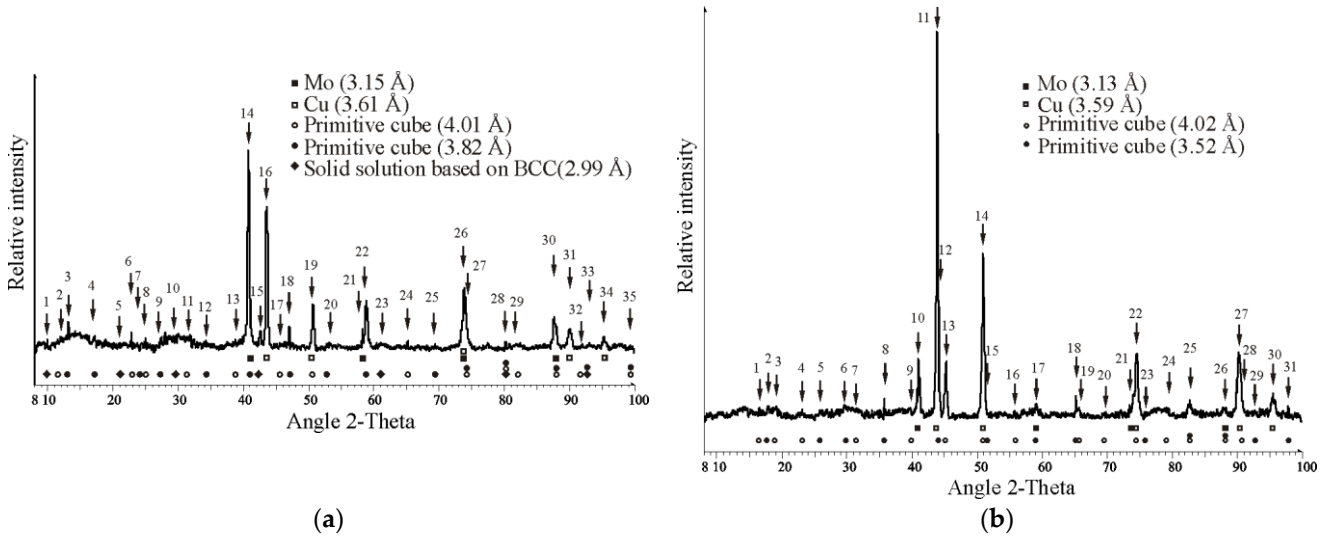

Figure 3. X–ray diffractogram of a composite material sample: (**a**)—from the molybdenum layer; (**b**)—from the copper layer.

It can be seen that in addition to the pure components (copper and molybdenum), a number of phases were detected in the samples: a solid solution based on molybdenum (BCC lattices) with a parameter of 2.99 Å and primitive cubic crystal lattices with a number of parameters (3.52, 3.82, 4.01, and 4.02 Å). It is important to note the peculiarity of the resulting picture, in which solid solutions based on the FCC lattice of copper are not observed, although copper is significantly more ductile than molybdenum.

Figure 4 shows an X-ray diffractogram of a sample of a copper plate after pressing a molybdenum plate on a press, from which it follows that completely different deformation conditions (first of all, the minimum specific pressure from all experiments) did not lead to any significant interaction of copper and molybdenum.

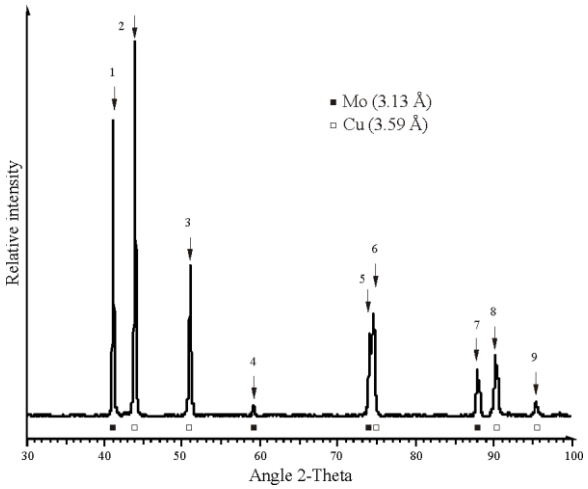

Figure 4. X-ray diffractogram from a copper plate after pressing a molybdenum plate into it on a press.

Figure 5 shows X-ray diffractograms of copper plate samples after pressing molybdenum wire into them on a press (experiments with wires 1 and 2).

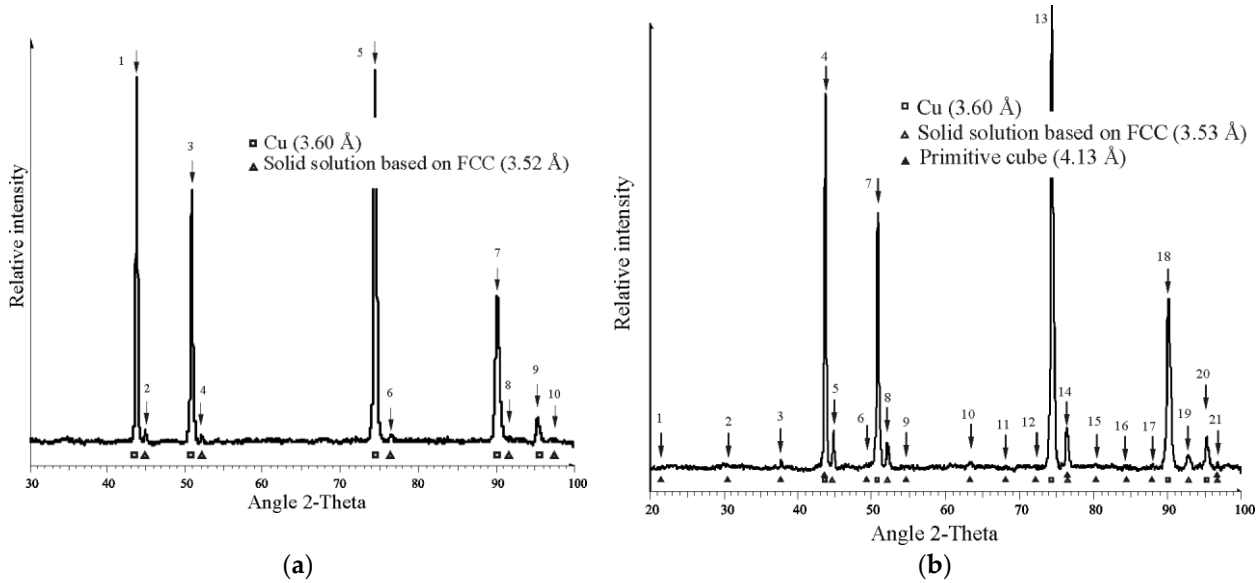

Figure 5. X–ray diffractograms from a copper plate after pressing a molybdenum wire into it on a press: (**a**)—experiment 2; (**b**)—experiment 1.

It can be seen from Figure 5 that the interaction conditions of copper and molybdenum strongly affect the resulting phase composition. So, in the case of experiment 2 (Figure 5a), where the area of the pressed molybdenum was significantly lower than in the case of pressing a molybdenum plate with the same force on the press (Figure 4), and therefore, the specific pressure was higher, in addition to pure copper, a solid solution based on a FCC lattice of copper was observed. In the second case (Figure 5b), the area of the pressed molybdenum wire was even lower. This led to the formation of not only a solid solution based on the FCC lattice but also to the appearance of a phase with a primitive cubic lattice with a parameter of 4.13 Å.

Studies of the microhardness of CMs after explosion welding have shown that the microhardness of the copper–molybdenum transition zone (where new phases are identified) has the highest values compared to areas remote from the transition zone (Figure 6).

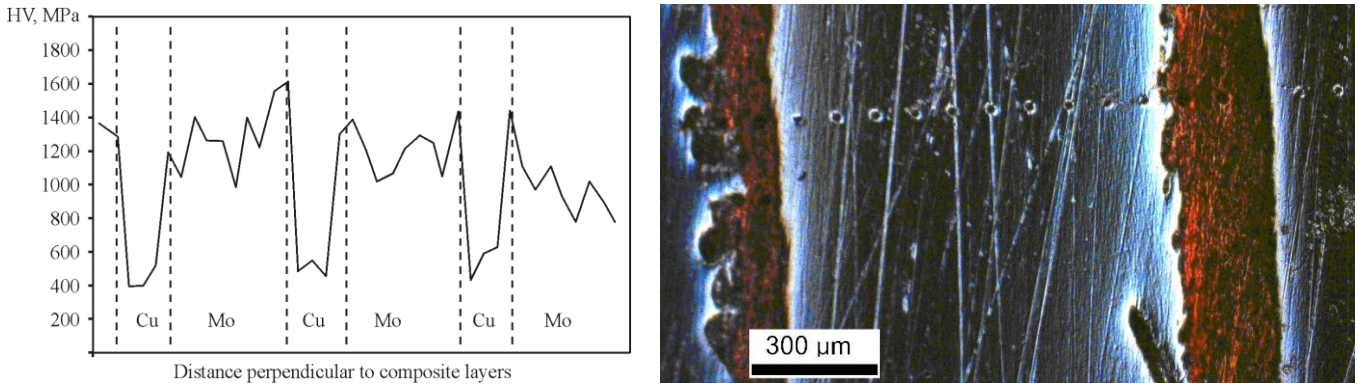

(**a**) (**b**)

Figure 6. Study of the microhardness of the composite: (**a**)—dependence of the microhardness values on the distance on a layered Cu–Mo sample; (**b**)—image of the connection zones of three layers of molybdenum and two layers of copper.

4. Discussion of the Results

Table 1 summarizes the phases identified after the interaction under pressure between copper and molybdenum. The table does not include pure components, copper and molybdenum, but they were found in all the relevant samples (see Figures 3–5). Recall the standard values of the parameters of crystal lattices: copper FCC a = 3.615 Å, and molybdenum BCC a = 3.147 Å.

Table 1. Summary table of identified phases in the copper–molybdenum system.

Type of Crystal Lattice	Crystal Lattice Parameter, Å	Experiment	The Experimental Data Are Presented
BCC	2.99	Explosion welding, molybdenum layer	Figure 3a
cP	3.82	Explosion welding, molybdenum layer	Figure 3a
cP	3.52	Explosion welding, copper layer	Figure 3b
cP	4.01	Explosion welding, molybdenum layer	Figure 3a
cP	4.02	Explosion welding, copper layer	Figure 3b
FCC	3.52	Mo wire pressed into Cu on the press (experiment 2) Mo wire	Figure 5a
FCC	3.53	Pressed into Cu on the press (experiment 1) Mo wire	Figure 5b
cP	4.13	Pressed into Cu on the press (experiment 1)	Figure 5b

It follows from Table 1 that a number of phases are formed in the copper–molybdenum system under pressure, which is explained by nonequilibrium interaction conditions. It can be seen that, during the interaction of the components, nonequilibrium phases were obtained by the type of solid solutions based on both the copper crystal lattice and the molybdenum crystal lattice. It should be kept in mind that the hardness of molybdenum is significantly higher than that of copper. This explains the distribution of these solid solutions. A solid solution based on a face-centered crystal lattice of copper ($a \approx 3.52$ Å, see Figure 5) formed during the experiment on the press with relatively small loads. In the case

of explosion welding during the interaction of copper and molybdenum, solid solutions based on a volume-centered molybdenum crystal lattice were identified (a = 2.99 Å, see Figure 3a). There was not enough energy for the formation of such a solid solution in the experiment on the press. In the case of explosion welding, a solid solution based on FCC copper turned out to be unstable, and, as will be shown, other phases arose instead.

The parameters of the obtained solid solutions attract attention; they are lower for both BCC and FCC than the parameters of molybdenum and copper, respectively. This may be due to the formation of not an ordinary solid solution but a superstructure, i.e., an atomically ordered solid solution in which copper and molybdenum atoms occupy not any but some definite position. The consequence of this may be the effect of superstructural compression. The confirmation of the formation of atomic ordering is the superstructural peaks of interference. For a solid solution based on a BCC lattice, these are indices of the types ($^1/_3$ 0 0) and ($^1/_2$ $^1/_2$ 0) (peaks 1 and 5 in Figure 3a).

To analyze other phases formed under extremely nonequilibrium conditions, it is necessary to involve the concept of tetrahedrally densely packed structures and cluster models of structure formation. In the existing cluster models of structure formation, transformation is described as the transition of the coordination polyhedron of the initial structure into another polyhedron of the final one [15,16]. For example, a cuboctahedron, i.e., the coordination polyhedron corresponding to the first coordination sphere of the densely packed FCC structure, can be transformed into an icosahedron (a Frank–Kasper polyhedron with 12 vertices), and the rhombododecahedron of the BCC structure can be transformed into a Frank–Kasper polyhedron with 14 vertices. An elementary act of structural transformation in these models is the displacement of the atoms of the original polyhedron by a distance less than the interatomic one. In [16], this position is described as the transfer of diagonals in a rhombus, which is the union of two triangular faces of a coordination polyhedron.

The cluster approach makes it possible to describe not only tetrahedrally densely packed phases but also ordinary crystal lattices, for example, FCC and HCP [12,15]. Such lattices can be described as combinations of tetrahedra and octahedra. According to [13], the FCC lattice can be represented as a combination of a regular octahedron surrounded by tetrahedra connected by common triangular faces (Figure 7a).

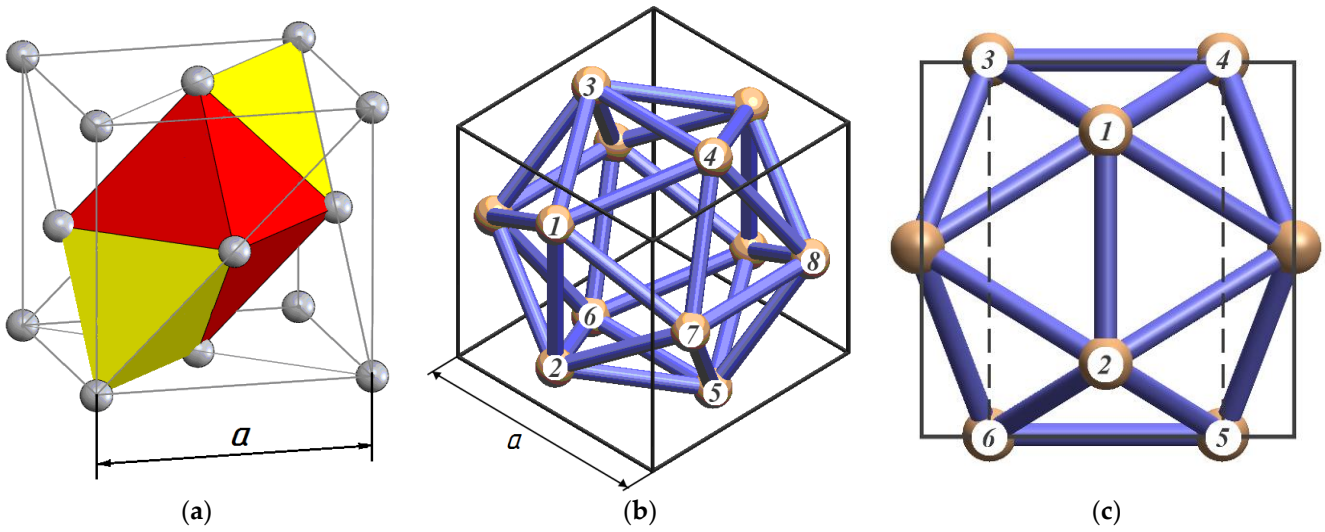

(**a**) (**b**) (**c**)

Figure 7. Cluster representation of crystal structures: (**a**)—rhombohedral cluster aggregate of the FCC lattice [13]; (**b**)—a diagram demonstrating the connection of the icosahedron with a primitive cubic lattice; (**c**)—a golden rectangle 3-4-5-6 in the icosahedron [32].

Table 1 shows that, along with bcc and FCC lattices, systems of reflections corresponding to a primitive cubic lattice with a number of parameters (3.82, 3.52, 4.01, and 4.13 Å) were discovered. To explain the appearance of such phases with such parameters, it was hypothesized that tetrahedral, close-packed structures based on icosahedral atomic configurations were formed in the structure.

Figure 6b shows how the icosahedron fits into the cube. To do this, edges of types 1-2, 3-4, or 7-8 are located in the faces of the cube. In an icosahedron, all edges are parallel in pairs, and each pair forms a golden rectangle, i.e., a rectangle with an edge ratio equal to 1.618 [32]. The golden rectangle is highlighted in Figure 7 in the dotted line as a 3-4-5-6 rectangle.

As shown in Figure 7, the FCC structure can be represented as a combination of an octahedron and a tetrahedron, and the edges of these figures are the same. For copper with a parameter a = 3.60 Å (see Figure 5b), the edge of the tetrahedron (d_{110} FCC lattice) will be 2.55 Å (for this, the parameter 3.60 Å must be divided by the root of two). Let us assume that an icosahedron is inscribed in a primitive cube with a parameter of 4.13 Å (see Table 1). The calculation of the length of its edges (and, accordingly, the edges of the 20 tetrahedra of which it consists) is performed by dividing the parameter 4.13 Å by the golden ratio of 1.618. The calculation result is 2.55 Å. The sizes of the tetrahedra folding the icosahedron coincide with the sizes of the tetrahedra forming the FCC copper structure. This explains the reason for the experimental detection of reflections corresponding to a primitive cube with a parameter of 4.13 Å (see Table 1). It is obvious that the "copper" tetrahedra under pressure formed not in the form of an FCC lattice but in the form of an icosahedron.

It should be noted that there are no atoms in the vertices of the primitive cube in Figure 7b. According to [12], a lattice with cubic symmetry may not contain atoms at the vertices of the cube, so the observed sets of reflexes of the cubic lattice will be extra reflexes, which by their nature differ from the superstructural reflexes caused by atomic ordering.

The study of the second identified primitive cube with a parameter of 4.01–4.02 Å (see Table 1) was carried out using the same logic. Let us assume that an icosahedron with an edge equal to the distance d_{110} = 2.50 Å of the FCC lattice (distance 1–2 and equivalent in Figure 7b) is inscribed in a cube with a primitive lattice parameter of 4.02 Å. The parameter a of this FCC lattice is 3.53 Å and corresponds to the solid solution found (Table 1). Checking the calculation consists of dividing the parameter 4.02 Å by 1.618, and the result is the desired value: 2.50 Å. Thus, rearranged tetrahedra of the FCC solid solution are observed here in the form of icosahedrons, which have formed another system of extra reflexes from a simple cubic lattice.

It is curious that solid solutions based on the FCC lattice were detected in an experiment made on a press, while the lattice of a primitive cube, indicating the formation of icosahedral atomic configurations, was found in an experiment during explosion welding (Table 1). It is likely that the possibilities of dissolving molybdenum in copper under pressure have some limitation, which, at relatively low pressures, manifests itself in the form of an "ordinary" solid solution based on a FCC lattice, and at high pressures—in the form of icosahedral configurations, but based on average tetrahedra of the same size as tetrahedra of an "ordinary" solid solution of FCC, obviously with the same amount of dissolved molybdenum.

In the experiment with explosion welding, two more phases with a primitive lattice are observed. A phase with a parameter of 3.82 Å was detected on the molybdenum layer and with a parameter of 3.52 Å on the copper layer. The reflexes of these phases are normal and not extra reflexes, as in the case of the other two primitive cubic lattices discussed above. This is confirmed by the very nature of the interference peaks, which for these two phases are very narrow, and where they do not overlap with the peaks of other phases, they are quite intense. This is clearly visible for a primitive lattice with a parameter of 3.82 Å in lines No. 4, 18, 25 (Figure 3a), and for a lattice with a parameter of 3.52 Å in lines No. 8, 18, 31 (Figure 3b). About the phases under consideration with a primitive lattice, we can say for sure that they consist of two types of atoms that form a superstructure, which is

confirmed by the presence of superstructural peaks (see Figure 3 in the region of small angles). It is interesting that the lattices of the primitive cube with a density of 52% arose during explosion welding and were not detected in the experiment with the press. This can be explained by differences in the energetics of the experiments. It is energetically easier to form icosahedral clusters from "ready-made" tetrahedra of an FCC lattice than to form a completely different primitive lattice; therefore, icosahedral phases were identified both in an experiment with explosion welding and in an experiment on a press, but in the latter case with the maximum specific pressure achieved.

The effect of moving atoms in solids over macroscopic distances in an extremely short time is known if we compare this phenomenon with diffusion [33]. For mass transfer caused by plastic deformation, the curvature of the crystal lattice and the emergence of new resolved structural states play an important role [33]. The interpenetration of dissimilar atoms can cause both a change in deformation properties (the Rebinder effect) and the development of chemical reactions, with the subsequent formation of a phase of this reaction [34].

The metal deformed during welding tends to dissipate energy, breaking up areas of inhomogeneous deformation into subdomains with its uniform distribution inside and changing from one subdomain to another. At the same time, all large-scale levels of the structure are involved. From nanocrystalline clusters (through the microscale level of crystal structure defects) and cluster conglomerates to meso- and macroscale levels, which include grains and their boundaries, as well as surfaces of solids [35,36]. Due to this, a strong welded joint is formed, with cluster layers of amorphized metal that contribute to the strengthening of localized zones (Figure 6).

5. Conclusions

It has been shown that during explosion welding of molybdenum and copper, self-organization of the structure occurs at various scale levels (component contact boundaries—grains—clusters). When deciphering X-ray diffraction patterns and microscopic methods, it was discovered that during the process of plastic deformation in the contact zone of the components, solid solution structures were formed at a depth of about 10 microns, based on both copper and molybdenum. In addition, it is shown that during explosion welding, it is possible to form atomic configurations with icosahedral symmetry, which are atomic assemblies of tetrahedral clusters corresponding to the identified solid solutions with cubic lattices based on copper. This became possible due to anomalously fast mass transfer and structure curvature localized at various scale levels. The study of microhardness made it possible to demonstrate that the copper–molybdenum contact zones, where amorphized metal phases with icosahedral symmetry were identified, have increased hardness. This is a promising opportunity to obtain composite materials with improved mechanical properties.

Author Contributions: Conceptualization, F.M.N. and L.I.K.; methodology, L.I.K. and V.I.M.; software, F.M.N. and R.Y.S.; validation, L.I.K. and F.M.N.; formal analysis, L.I.K.; investigation, L.I.K. and V.I.M.; resources, M.A.E. and R.Y.S.; data curation, F.M.N.; writing—original draft preparation, M.A.E.; writing—review and editing, F.M.N. and L.I.K.; visualization, F.M.N.; supervision, L.I.K.; project administration, F.M.N.; funding acquisition, F.M.N. and L.I.K. All authors have read and agreed to the published version of the manuscript.

Funding: This research received no external funding.

Data Availability Statement: Not applicable.

Acknowledgments: The authors express their gratitude to Artur K. Abkaryan (Siberian Federal University, Krasnoyarsk, Russia) for his help in conducting the experiment.

Conflicts of Interest: The authors declare no conflict of interest.

References

1. Lyakishev, N.P. (Ed.) *Diagrams of the State of Double Metal Systems: Reference Book: In 3 Volumes*; Mechanical Engineering: Moscow, Russia, 1997; Volume 2. (In Russian)
2. Kerber, M.L. Composite materials. *Soros Educ. J.* **1999**, *5*, 33–41. (In Russian)
3. Meng, X.; Huang, Y.; Cao, J.; Shen, J.; dos Santos, J.F. Recent progress on control strategies for inherent issues in friction stir welding. *Prog. Mater. Sci.* **2020**, *115*, 100706. [CrossRef]
4. Kolařík, L.; Janovec, J.; Kolaříková, M.; Nachtnebl, P. Influence of Diffusion Welding Time on Homogenous Steel Joints. *Procedia Eng.* **2015**, *100*, 1678–1685. [CrossRef]
5. Shan, S.; Liu, Y.; Zhang, J.; Fan, X.; Jiao, K. Explosion welding research on large-size ultra-thick copper-steel composites: A review. *J. Mater. Res. Technol.* **2023**, *24*, 4130–4142. [CrossRef]
6. Lysak, V.I.; Kuzmin, S.V. *Explosion Welding*; Mashinostroenie: Moscow, Russia, 2005. (In Russian)
7. Deribas, A.A. *Physics of Hardening and Explosion Welding*; Novosibirsk: Nauka, Russia, 1972. (In Russian)
8. Oglezneva, S.A.; Dolivets, O.V. Investigation of the structure and properties of electrodes-tools made of Pseudo-alloys based on copper. *Master's J.* **2014**, *2*, 25–33, No. 2., EDN THAJSL.
9. Sakenova R., Y. Method of Vacuum-Arc Ion-Plasma Deposition of a Solid Coating. KZ Patent No. 3472, 20 November 2020.
10. Kraposhin, V.S. Assembling an icosahedral quasicrystal from hierarchical atomic clusters. *Crystallography* **1996**, *41*, 395–404. (In Russian)
11. Yeletsky, A.V.; Smirnov, B.M. Properties of cluster ions. *Physics–Uspekhi* **1989**, *32*, 763–782. [CrossRef]
12. Pearson, W.B. *The Crystal Chemistry and Physics of Metals and Alloys*; Wiley-Interscience: London, UK, 1972; 806p.
13. Bulenkov, N.A.; Tytik, D.L. Modular design of icosahedral metal clusters. *Russ. Chem. Bull.* **2001**, *50*, 1–19. (In Russian) [CrossRef]
14. Rudman, P.S.; Stringer, J.; Jaffee, R.I. *Phase Stability in Metals and Alloys: Battelle Institute Materials Science Colloquia, Geneva and Villars, Switzerland. March 7–12, 1966*; McGraw-Hill: New York, NY, USA, 1967.
15. Bulenkov, N.A. *Substantiation of the Concept of "Crystal Module"*; Solid State Physics Series; Vestnik of Lobachevsky State University of Nizhni Novgorod: Nizhny, Russia, 1998; pp. 19–30. (In Russian)
16. Kraposhin, B.C.; Silchenkov, A.D. Crystallographic mechanism of perlite transformation in the iron-carbon system. *Probl. Ferr. Metall. Metallol.* **2009**, *2*, 55–64. (In Russian)
17. Shechtman, D.; Blech, I.; Gratias, D.; Cahn, J.W. Metallic Phase with Long-Range Orientational Order and No Translational Symmetry. *Phys. Rev. Lett.* **1984**, *53*, 1951–1953. [CrossRef]
18. Gratias, D. Les quasi-cristaux. *La Rech.* **1986**, *178*, 788–798. (In French)
19. Krasnov, V.Y.; Poletaev, G.M.; Starostenkov, M.D. Investigation of the structure of amorphous nickel. *Fundam. Probl. Mod. Mater. Science.* **2006**, *3*, 37–45. (In Russian)
20. Kraposhin, V.; Talis, A.; Samoylovitch, M. Axial (helical) substructures determined by the root lattice E8 as generating clusters of the condensed phases. *J. Non-Cryst. Solids* **2007**, *353*, 3279–3284. [CrossRef]
21. Frank, F.C.; Kasper, J.S. Complex alloy structures regarded as sphere packings. I. Definitions and basic principles. *Acta Crystallogr.* **1958**, *11*, 184–190. [CrossRef]
22. Frank, F.C.; Kasper, J.S. Complex alloy structures regarded as sphere packings. II. Analysis and classification of representative structures. *Acta Crystall.* **1959**, *1*, 483–499. [CrossRef]
23. Mai, Z.H.; Xu, L.; Wang, N.; Kuo, K.H.; Jin, Z.C.; Cheng, G. Effects of phason strain on the transition of an octagonal qusicrystal to a β–Mn–type structure. *Phys. Rev. B* **1989**, *40*, 183–186. [CrossRef]
24. Ivanov, E.Y.; Konstanchuk, I.G.; Bokhonov, B.B.; Boldyrev, V.V. Mechanochemical synthesis of icosahedral phases in Mg–Zn–Al and Mg–Cu–A1 alloys. *React. Solids* **1989**, *7*, 167–172. [CrossRef]
25. Scudino, S.; Surreddi, K.B.; Sager, S.; Sakaliyska, M.; Kim, J.S.; Löser, W. Production and mechanical properties of metallic glass-reinforced Al-based metal matrix composites. *J. Mater. Science.* **2008**, *43*, 4518–4526. [CrossRef]
26. Konstanchuk, I.; Ivanov, E.; Bokhonov, B.; Boldyrev, V. Hydriding properties of mechanically alloyed icosahedral phase $Ti_{45}Zr_{38}Ni_{17}$. *J. Alloys Compd.* **2001**, *319*, 290–295. [CrossRef]
27. Eckert, J.; Schultz, L.; Urban, K. Formation of quasicrystals by mechanical alloying. *Appl. Phys. Lett.* **1989**, *55*, 117–119. [CrossRef]
28. Kveglis, L.I.; Noskov, F.M.; Volochaev, M.N.; Nyavro, A.V.; Filarowski, A. Magnetic Properties of Nickel-Titanium Alloy during Martensitic Transformations under Plastic and Elastic Deformation. *Symmetry* **2021**, *13*, 665. [CrossRef]
29. Kveglis, L.; Abylkalykova, R.; Noskov, F.; Arhipkin, V.; Musikhin, V.; Cherepanov, V.; Niavro, A. Local electron structure and magnetization in β-Fe86Mn13C. *Superlattices Microstruct.* **2009**, *46*, 114–120. [CrossRef]
30. Kveglis, L.I.; Makarov, I.N.; Noskov, F.M.; Nasibullin R., T.; Nyavro, A.V.; Cherepanov V., N.; Olekhnovich A., E.; Saprykin, D.N. Magnetic characteristics of iron nanoclusters. *Sib. Aerosp. J.* **2021**, *22*, 526–535. [CrossRef]
31. Mali, V.I.; Pavliukova, D.V.; Bataev, I.A.; Bataev, A.A.; Smirnov, A.I.; Yartsev, P.S.; Bazarkina, V.V. Formation of the Intermetallic Layers in Ti-Al Multilayer Composites. *Adv. Mater. Res.* **2011**, *311–313*, 236–239. [CrossRef]
32. Kraposhin, V.S. Golden section in the structure of metals. *Mater. Sci. Heat Treat. Met.* **2005**, *47*, 351–358. (In Russian) [CrossRef]
33. Panin, V.E.; Egorushkin, V.E. Curvature solitons as generalized wave structural carriers of plastic deformation and destruction. *Phys. Mesomech.* **2013**, *16*, 7–26. (In Russian) [CrossRef]
34. Boldyrev, V.V. Mechanochemistry and mechanical activation of solids. *Uspekhi Khimii* **2006**, *75*, 203–216. (In Russian) [CrossRef]

35. Panin, V.E.; Panin, V.E.; Likhachev, V.A.; Grinyaev, Y.V. *Structural Levels of Deformation of Solids*; Yanenko, N.N., Ed.; Siberian Branch Nauka: Novosibirsk, Russia, 1985; 229p. (In Russian)
36. Panin, V.E.; Egorushkin, V.E. Fundamentals of physical mesomechanics of plastic deformation and destruction of solids as nonlinear hierarchically organized systems. *Phys. Mesomech.* **2015**, *18*, 100–113. (In Russian) [CrossRef]